5-8-1989

Origins of the Quantum Efficiency Duality In the Primary Photochemical Event of Bacteriorhodopsin

Robert R. Birge
Syracuse University

Leonore A. Findsen
Syracuse University

Albert F. Lawrence
Syracuse University

Mark Masthay
University of Dayton, mmasthay1@udayton.edu

Chian-Fan Zhang
Syracuse University

Origins of the Quantum Efficiency Duality in the Primary Photochemical Event of Bacteriorhodopsin

Robert R. Birge, Leonore A. Findsen, Albert F. Lawrence, Mark B. Masthay and Chian-Fan Zhang

Department of Chemistry and Center for Molecular Electronics
Syracuse University, Syracuse, New York 13244-1200 USA

ABSTRACT

Experimental and theoretical evidence is presented which suggests that two distinct forms of light-adapted bacteriorhodopsin may exist. We propose that these two forms have characteristic photocycles with significantly different primary quantum yields. INDO-PSDCI molecular orbital procedures and semiempirical molecular dynamics simulations predict that one ground state geometry of bR undergoes photochemistry with a primary quantum yield, Φ_1, of ~ 0.27, and that a second ground state geometry, with a slightly displaced counterion, yields Φ_1 ~ 0.74. This theoretical model is supported by the observation that literature measurements of Φ_1 tend to fall into one of two categories- those that observe Φ_1 ~ 0.33 or below, and those that observe Φ_1 ~ 0.6 or above. The observation that all photostationary state measurements of the primary quantum yield give values near 0.3, and all direct measurements of the quantum yield result in values near 0.6, suggests that photochemical back reactions may select the bacteriorhodopsin conformation with the lower quantum yield. The two photocycles may have developed as a natural biological requirement that the bacterium have the capacity to adjust the efficiency of the photocycle in relation to the intensity of light and/or membrane electrochemical gradient.

1. INTRODUCTION

Bacteriorhodopsin is the light-harvesting protein of the purple membrane of the halophilic microorganism *Halobacterium halobium*.[1-4] This 26,000 molecular weight protein is grown by the bacterium under conditions of oxygen deprivation, when the normal respiration process of using oxygen to synthesize ATP becomes too inefficient to sustain growth. The role of the bacteriorhodopsin is to convert light energy into a hydrogen ion gradient that chemiosmotically drives the synthesis of ATP. Unlike the visual pigment rhodopsin, which undergoes a photobleaching sequence and ejects the retinal chromophore, bacteriorhodopsin undergoes a photocycle which returns the activated protein to its original state. There are obvious biological advantages to a photocycle versus a photobleaching sequence, not the least of which is a significant gain in the overall system efficiency associated with a self-resettable system. Given the inefficiency and complexity of the visual rhodopsin system, which requires enzymatic intervention to reisomerize the chromophore prior to regeneration of the protein, it is interesting to speculate on why natural selection would adopt complexity over simplicity. The apparent answer is the requirement that the visual system have a mechanism of adjusting to different light intensities. By having a relatively slow pigment regeneration process, the visual system adjusts the sensitivity of the receptor surface as a function of light flux. A question that remains to be answered is how *Halobacterium halobium* adjusts the efficiency of the proton pumping system as a function of light intensity and/or membrane electrochemical gradient. In this paper we will investigate the possibility that the quantum efficiency, as well as the energy storage capacity, of bacteriorhodopsin are coupled, two-level adjustable parameters that can be modified to optimize the performance of the proton pump. This capability may have developed via natural selection so that a photocycling system, inherently lacking the sensitivity feedback mechanism associated with a bleaching sequence, would have the internal capacity to adjust to external conditions.

We present in this paper molecular dynamics simulations of the primary event of bacteriorhodopsin which indicate that a small shift in the location of the primary counterion relative to the protonated Schiff base linkage can produce a dramatic change in the quantum efficiency of the bR→K photoreaction. Our simulations find experimental support in (and provide a mechanistic explanation for) the observation that experimental measurements tend to yield Φ_1 ~ 0.3 or Φ_1 ~ 0.6, while excluding intermediate values.

2. METHODS

2.1 Binding site model

Our model of the active site of light adapted bacteriorhodopsin (**bR**) is shown in Fig. 1a. We assume that the primary counterion is the aspartic acid residue (ASP_{212}) that is located one helical turn away from the lysine residue (LYS_{216}) to which the retinyl chromophore is covalently bound. While some investigators argue for a pair of charges near the β-ionylidene ring[5-7], our two-photon investigations of light adapted bacteriorhodopsin indicate that these charges, if present, have a very small effect on the electronic structure of the polyene chromophore.[8] Thus, we have not included these charges in our simulations. We assume that the primary event involves a 13-*trans* to 13-*cis* photoisomerization to produce **K** (Fig. 1b). While multi-bond photoisomerization models have been proposed,[9-12] recent Raman[13] and photostationary state[14] spectroscopic studies support the simple, one-bond photoisomerization shown in Fig. 1.

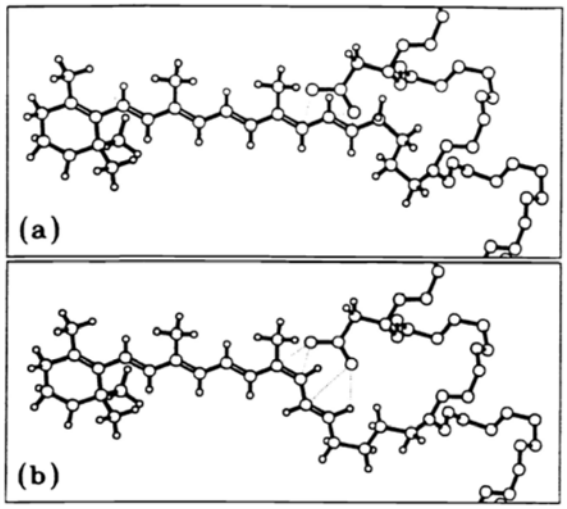

Figure 1. The assumed structure of the binding site of light adapted bac-teriorhodopsin is shown in (a), and the assumed structure of the primary photoproduct, **K**, is shown in (b). These two structures will be labelled $\mathbf{bR_1}$ and $\mathbf{K_1}$, and yield the potential surfaces and excited state trajectories shown in the left rectangle in Fig. 2. An alternative pair of structures, labelled $\mathbf{bR_2}$ and $\mathbf{K_2}$ can be generated by moving the entire chromophore away from the counterion by a slight rotation of the entire polyene chromophore about the β-γ lysine bond. This rotation decreases electrostatic stabilization of the all-*trans* chromo-phore in $\mathbf{bR_2}$ and results in a smaller amount of energy storage in the primary photoproduct $\mathbf{K_2}$.

2.2 Molecular orbital methods

Molecular orbital calculations were carried out by using the all-valence electron INDO-PSDCI procedures described in Refs. 15-17. All single excitations below 15eV and all double excitations below 20eV were included in the CI Hamiltonian for the excited state calculations. These energy constraints generated a CI Hamiltonian containing ~350 single and ~750 double valence excitations for the model bacteriorhodopsin systems investigated here. Transitions from the counterion to the chromophore were explicitly excluded from the CI Hamiltonian in a majority of calculations to limit the size of the CI matrix as well as the final state distribution. These charge transfer states result in low-lying, optically forbidden (or very weak) transitions which do not mix appreciably with the chromophore valence transitions.[15,18] Test calculations indicate that the exclusion of charge transfer states does not diminish unduly the accuracy of the valence state calculations. This exclusion saves considerable computation time and was necessary for generating the partially optimized surfaces used in the molecular dynamics calculations.

2.3 Molecular dynamics methods

Molecular dynamics calculations were carried out by using the semiclassical procedures described in Refs. 16 and 17 and reviewed in 19. Our ground and excited state surfaces are defined in reference to the principal torsional coordinate [$\tau(C_{12}-C_{13}=C_{14}-C_{15})$] and were generated by adiabatic minimization of all labile lysine internal coordinates as well as the following polyene stretching (R), bending (<), and torsional (τ) coordinates: $R(C_{11}=C_{12})$, $R(C_{12}-C_{13})$, $R(C_{13}=C_{14})$, $R(C_{14}-C_{15})$, $R(C_{15}=N_{16})$, $<(C_{11}=C_{12}-C_{13})$, $<(C_{12}-C_{13}=C_{14})$, $<(C_{13}=C_{14}-C_{15})$, $<(C_{14}-C_{15}=N_{16})$, $\tau(C_{10}-C_{11}=C_{12}-C_{13})$, $\tau(C_{11}=C_{12}-C_{13}=C_{14})$, $\tau(C_{12}-C_{13}=C_{14}-C_{15})$, and $\tau(C_{13}=C_{14}-C_{15}=N_{16})$. The location of the counterion, the entire β-ionylidene ring and the lysine residue atoms fixed via attachment to the α-helix were (arbitrarily) held stationary during the isomerization. This was a required constraint because these degrees of freedom were manipulated to best reproduce the experimental spectroscopic and energetic properties. All dynamics were carried out by using Lagrangian interpolation on the ground and excited state surfaces to define the steepest decent gradients (see Appendix of Ref. 17). The equations of motion were solved and the positions of the nuclei updated in temporal increments of 0.1 fsec. The probability of crossing from the excited state into the ground states was calculated by using the semiclassical S matrix methods of Miller and George[20] as modified by Birge and Hubbard.[16-17] While these methods are approximate, identical methods were used to simulate rhodopsin photochemistry, and the calculated quantum yields (Φ_1=0.62, Φ_2=0.48) were in reasonable agreement with the observed values (Φ_1=0.67, Φ_2=0.49) (see discussion in Ref. 19).

3. RESULTS

Our calculations are an extension of the calculations reported originally in Ref. 21, and our results are summarized in Fig. 2. The molecular dynamics simulations predict complex dynamics and biphasic repopulation of the ground state following excitation of **bR**. The calculations shown in the left rectangle are reproduced from Ref. 21 and are based on the binding site model shown in Fig. 1. Roughly one-third of the excited molecules are trapped in an excited state potential well, and decay back to the ground state via non-dynamic processes. The simulations predict that this S_1^* potential well has a 13-transoid minimum so that decay of those species trapped in this well preferentially regenerate **bR**. The ground state conformation of **bR** (referred to as $\mathbf{bR_1}$) assumed in the calculations shown on the left was optimized to reproduce as accurately as possible the optical and photocalorimetric data at 77K. The calculations shown in the rectangle at right were carried out by allowing for a smaller amount of energy storage in the primary event and arbitrarily moving the entire chromophore away from the counterion by rotating about the β-γ lysine bond (Fig. 1a). This change decreases electrostatic stabilization of the all-trans chromophore, and shifts the S_1^* potential well to a 13-cisoid conformation. We refer to this geometry as $\mathbf{bR_2}$. The molecular dynamics calculations predict that roughly one-third of the $\mathbf{bR_2}$ molecules excited into the lowest singlet state are trapped in this S_1^* potential well and preferentially decay to form product (**J** or **K**). (For the purposes of this discussion, we are treating **J** and **K** as similar species with respect to chromophore geometry with both species possessing ground state 13-cis geometries. The possibility that **J** is an excited state species, however, has been proposed.[21]) The calculations predict that a small change in ground state geometry produces a dramatic increase in the primary quantum yield [$\Phi_1(\mathbf{bR_1}) = 0.266$; $\Phi_1(\mathbf{bR_2}) = 0.743$]. Because the probability of coupling into the ground state is relatively low for each trajectory (average crossing probability is less than 10% for the first ten passes over the orthogonal crossing region), the quantum yield sums are very close to unity for both geometries [$(\Phi_1 + \Phi_2)(\mathbf{bR_1}) = 1.004$; $(\Phi_1 + \Phi_2)(\mathbf{bR_2}) = 1.02$]. Although the $\mathbf{bR_2}$ geometry is calculated to have a higher chromophore-counterion energy (~2 kcal mol^{-1}) relative to the $\mathbf{bR_1}$ geometry (based on the binding site model of Ref. 25), the $\mathbf{bR_2}$ geometry may be more stable when the entire protein energy is taken into account.

Our theoretical results can be summarized as follows. There are two forms of light adapted bacteriorhodopsin which have very similar geometries, ground state energies and spectroscopic properties, but significantly different photochemical and energy storage characteristics. Because our model of the binding site and our theoretical procedures are approximate, it is important that our results be viewed as illustrative rather than rigorously accurate. The issue that will be addressed in the following section is the extent to which our theoretical predictions provide insights into the observed spectroscopic and photochemical properties of bacteriorhodopsin.

4. DISCUSSION

The subsequent discussion will seek to answer the following three questions. First, is there experimental evidence in support of our theoretical prediction that there are two forms of bacteriorhodopsin ($\mathbf{bR_1}$ and $\mathbf{bR_2}$) with significantly different primary quantum yields? Second, if such an observation has experimental support, what are the key variables that are responsible for selecting $\mathbf{bR_1}$ versus $\mathbf{bR_2}$? Third, what is the biological relevance of two forms of **bR** with the properties assigned in Fig. 2?

4.1 Experimental evidence of a quantum yield duality

Despite extensive experimental study,[22-32] assignment of the primary photochemical quantum yield of light-adapted bacteriorhodopsin remains a subject of controversy. As can be seen by reference to Table I, measurements of Φ_1 range from a low of 0.25 to a high of 0.79. This measurement range is in sharp contrast to the agreement that is observed in the literature with respect to the measurement of the primary quantum yield for vertebrate rhodopsin photochemistry.[33-35] A closer examination of the data presented in Table I indicates that all of the experimental measurements fall into one of two categories- those that predict $\Phi_1 = 0.33$ or below and those that predict $\Phi_1 = 0.6$ or above. No experimental measurements fall into the large intermediate range spanning from 0.34 - 0.59. If experimental uncertainty were the dominant source of the discrepancies in the measured quantum yields, one would predict that a majority of the measurements would fall into this intermediate range in contrast to none at all. Thus, the data in Table I supports the concept that there are two types of bacteriorhodopsin, one that has a forward quantum yield of approximately 0.3 and a second that has a forward quantum yield of approximately 0.6. Before we accept this interpretation, however, it is important to consider alternative explanations that may be responsible for producing systematic errors capable of generating an apparent duality.

Kouyama *et al.* have examined the influence of the **N** intermediate on the bacteriorhodopsin photocycle.[36] The **N** intermediate has a major absorption maximum very close to that of bacteriorhodopsin and is photoactive. Kouyama *et al.* propose that at high pH and high light intensity, the overall photoreaction of bacteriorhodopsin may be approximated by the two-photon cycle,

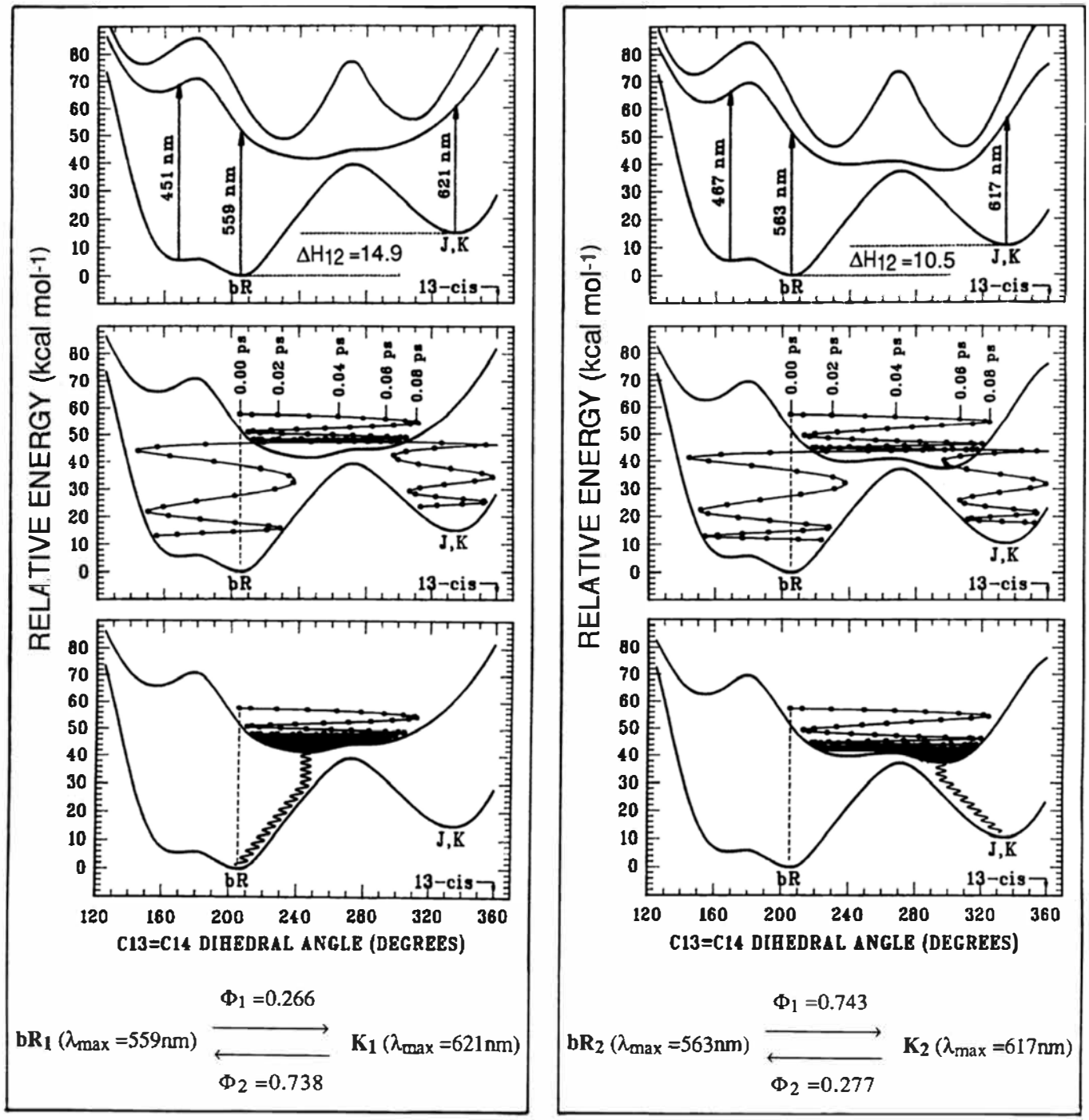

Figure 2. Molecular dynamics of the primary photochemical transformation of light adapted bacteriorhodopsin based on two different models of the binding site. The calculations shown in the left rectangle ($bR_1 \rightarrow K_1$) are reproduced from Ref. 21 and are based on the binding site model shown in Fig. 1. The calculations shown in the rectangle at right ($bR_2 \rightarrow K_2$) were carried out by allowing for a smaller amount of energy storage in the primary event by arbitrarily displacing the entire chromophore away from the counterion by rotating about the β-γ lysine bond (see text).

$$\mathbf{bR} \xrightarrow{h\nu} \mathbf{K} \rightarrow \mathbf{L} \rightarrow \mathbf{M} \rightarrow \mathbf{N} \xrightarrow{h\nu} (^{N}\mathbf{L} \Leftrightarrow {}^{N}\mathbf{M}) \rightarrow \mathbf{bR},$$

whereas at neutral pH and low light intensity, it can be described by the one-photon cycle

$$\mathbf{bR} \xrightarrow{h\nu} \mathbf{K} \rightarrow \mathbf{L} \rightarrow \mathbf{M} \rightarrow \mathbf{N} \rightarrow \mathbf{O} \rightarrow \mathbf{bR}.$$

Thus, the above two schemes could account for anomalies in quantum yield measurements at ambient temperatures involving the observation of **M**. For example, the presence of the two-photon cycle would artificially decrease the measured quantum yield of **M** formation by up to one-half. Thus, if we assume Φ_1 ~0.6, a continuous wave experimental measurement at high pH and high light intensity could yield ~0.3, because roughly half of the photons absorbed would be absorbed by **N**, which has an absorption spectrum very similar to **bR**. While it is possible that some of the measurements reported in Table I might have been affected by this effect, a majority of the measurements reported in Table I do not. Thus, we must seek alternative explanations.

Table I. Literature Assignments of the Primary Quantum Yields of Light Adapted Bacteriorhodopsin.

Investigators[a]	Φ_1[b]	Φ_2[c]	Φ_1/Φ_2	$\Phi_1+\Phi_2$	T[d]	Reaction[d]	Conditions[e]
O&H (1973)	**0.79**[f]	—	(>0.78)	—	300	**bR→M**	HS/ether
GOK (1976)	—	—	**0.40**	—	300	**bR⇔K**	aqueous
B&E (1977)	**0.30±0.03**	**0.77±0.12**	0.39±0.15	1.07±0.15	233	**bR⇔M**	glycerol
GKRO (1977)	**0.25±0.05**	**0.63±0.20**	0.40±0.18	0.88±0.25	300	**bR⇔K**	aqueous
H&E (1978)	**0.33±0.05**	**0.67±0.04**	0.49±0.10	1.00±0.09	77	**bR⇔K**	glycerol
OHT (1985)	**>0.6**	—	(>0.6)	—	300	**bR→M**	HS/ether
P *et al.* (1986)	**~0.6**	—	(≥0.6)	—	300	**bR→K**	aqueous
DSTC (1988)	**0.31±0.10**	**0.93±0.14**	0.33±0.15	1.24±0.24	296	**bR⇔K**	aqueous
B *et al.* (1989)	<0.49	—	**0.45±0.03**	<1.48	77	**bR⇔K**	glycerol

(a) Investigators are defined as follows:
GOK(1976) = Goldschmidt *et al.* (Ref. 25),
GKRO(1977) = Goldschmidt *et al.* (Ref. 24),
OHT(1985) = Oesterhelt *et al.* (Ref. 27),
DSTC (1988) = Dioumaev *et al.* (Ref. 32),
O&H(1973) = Oesterhelt and Hess (Ref. 29),
B&E(1977) = Becher and Ebrey (Ref. 26),
H&E(1978) = Hurley and Ebrey (Ref. 23),
P *et al.*(1986) = Polland *et al.* (Ref. 28),
B *et al.*(1989) = Birge et al. (Ref. 14).

(b) Quantum yield for the formation of the primary photoproduct, **K**, from **bR**. Some investigators assigned this value by measuring the quantum yield of the **bR→M** photoreaction and by assuming that the quantum yield for the **bR→M** photoreaction is identical to that for the **bR→K** reaction (i.e., no branching back to **bR** occurs during the dark steps). The individual references should be consulted for error range assignments.

(c) Quantum yield for the formation of **bR** from the primary photoproduct, **K**. Some investigators assigned this value by measuring the quantum yield of the **M→bR** photoreaction and by assuming that the quantum yield for the **M→bR** photoreaction is identical to that for the **K→bR** reaction. The individual references should be consulted for error range assignments.

(d) The measurement temperature (in Kelvin) and the photoreaction studied. The symbol "⇔" is used to represent a photostationary state measurement.

(e) Solvent conditions used in the experimental measurement. When specific solvent conditions are not provided, "aqueous" is assumed. HS represents high salt, and "glycerol" conditions are typically mixtures of glycerol and water. Individual references should be consulted for more detailed descriptions of the experimental conditions.

(f) Values shown in boldface were measured directly and the error ranges, when reported, are those provided by the investigators. Remaining values in the same row were derived from the data in boldface.

A cursory examination of Table I suggests that temperature might be responsible for generating a decreased forward quantum yield. This is an important possibility to investigate, because a small barrier in the excited state potential surface, rather than two forms of bacteriorhodopsin, could be the source of the observed duality. Indeed, isorhodopsin photochemistry displays a temperature dependent quantum yield due to a very small barrier in the excited state.[15] While it is true that all of the measurements resulting in values of $\Phi_1 \geq 0.6$ were carried out at ambient temperature, three ambient temperature measurements yielded values in the range 0.25-0.31. Thus, temperature is not uniquely responsible for generating the large differences in Φ_1.

Two of the three ambient temperature measurements generating values of $\Phi_1 > 0.6$ were carried out by measuring the formation of **M** in high salt, ether solution. Ether is known to increase the lifetime of the **M** intermediate,[26,29] although the mechanism is not understood. It is also known that salt concentration has a dramatic effect on the quantum yield of proton translocation.[37-40] Recent investigations suggest that the nature of the photocycle is dramatically affected by pH.[41,42] These latter studies suggest that there are at least two independent photocycles for light adapted bacteriorhodopsin, one which is responsible for generating M_{fast}, and a second which is responsible for generating M_{slow}. A third photocycle may be responsible for generating the recently observed intermediate called **R**.[42,43] Thus, a distribution of photocycles may exist. There is additional information that supports the concept of at least two photocycles. A number of investigators have proposed the presence of branching points and/or parallel pathways in the photocycle.[44-47] Hanamoto *et al.* proposed that there are two forms of **M** that are alternately populated depending upon the ionization state of an apoprotein moiety with a pK near 9.6.[41] Iwasa *et al.*[31] and Balashov and Litvin[48] have proposed the existence of two forms of **K**. Similarly, Stockburger *et al.* have proposed the existence of two forms of **L**.[49] All of these observations are consistent with the concept of two (or more) photocycles. The proposal that there are two different photocycles is not identical to a proposal that there are two different forms of bacteriorhodopsin, each with a characteristic photocycle. In principal, it is possible that there is only one form of **bR**, and that the two photocycles share a common **bR**. This interpretation is unlikely, however, given the observation of different **bR** $\rightarrow$**K** quantum yields (Table I), because the molecular changes associated with the primary event are believed to be localized within the retinyl chromophore.

A key observation that can be made by reference to Table I is that all photostationary state measurements yield values of Φ_1 near 0.3 and all direct measurements yield values of Φ_1 near 0.6. It is therefore tempting to propose that there is some systematic error that is affecting one type of measurement, but not the other. While this explanation cannot be ruled out, it is very unlikely. Photostationary state measurements on rhodopsin yield results identical to those obtained via direct measurements (see Ref. 35). A careful reading of those papers listed in Table I that predict Φ_1 near 0.6 indicates that the investigators took care to avoid systematic errors of the type that might overestimate the primary quantum yield. This observation is particularly relevant to those direct measurements reported after 1984, because the investigators recognized that their measurements conflicted with a large number of prior studies that yielded Φ_1 near 0.3. We conclude that systematic errors are very unlikely to be responsible for the observed duality in the experimental measurements of the primary quantum yield.

4.2 Photophysical origins of the quantum yield duality

The analysis of the previous section provides evidence that there are two forms of bacteriorhodopsin, each with a characteristic photocycle. We will adopt the labels $\mathbf{bR_1}$ and $\mathbf{bR_2}$ to indicate these two forms, following the theoretical model presented in Figs. 1 and 2. In this section we will explore the possible external stimuli that may be responsible for preferentially selecting one form over the other.

Analysis of the data of Table I suggests that whatever perturbation is responsible for preferentially selecting $\mathbf{bR_1}$ versus $\mathbf{bR_2}$, it is difficult, if not impossible, to populate both forms simultaneously. Otherwise, we would observe quantum yield values characteristic of averages of $\mathbf{bR_1}$ and $\mathbf{bR_2}$. As discussed in the previous section, solvent, temperature, ionic strength and pH may affect the distribution of these photocycles in a complex way that remains to be explored in detail. However, it is difficult to rationalize why any of these environmental perturbations would force population of one form of **bR** versus another and avoid the generation of a thermodynamic equilibrium containing both.

We suggest the possibility that photochemistry, rather than environment, may be the key selector of photocycle. This proposal is based on the observation that *all* direct experimental measurements on Φ_1 yield values greater than or equal to 0.6, while *all* photostationary state measurements on Φ_1 yield values less than or equal to 0.33. This observation suggests a dual photocycle system as depicted in Fig. 3. The thick arrows in this figure indicate photochemical transformations while the thin arrows indicate thermal transformations. Thus, the $\mathbf{bR_2}$ photocycle, which has the higher primary quantum yield, is the thermally more stable. Direct measurements will yield high values for Φ_1, because the $\mathbf{bR_2}$—$h\nu\rightarrow$ $\mathbf{K_2}$ photoreaction will be selected. However, the back reaction is not $\mathbf{K_2}$—$h\nu\rightarrow\mathbf{bR_2}$ but rather $\mathbf{K_2}$—$h\nu\rightarrow\mathbf{bR_1}$. Subsequent photochemistry will take place within the $\mathbf{bR_1}$ photocycle, which will select the

bR_1—hν→K_1 reaction, and yield a lower primary quantum yield. Because the reverse photoreaction from K_1 also selects bR_1, all photostationary measurements will measure the bR_1—hν→K_1 quantum yield, which is ~0.3.

It is possible that a change in the ionization state of a group on the apoprotein, rather than a change in the chromophore-counterion geometry (Fig. 2), is responsible for transforming bR_1 to bR_2. The recent studies of El-Sayed and coworkers[41] provide support for this alternative hypothesis. These investigators proposed that the biphasic kinetics observed in the formation of **M** are associated with two different chromophore environments provided by the apoprotein.[41] They proposed further that the two forms are alternately populated depending upon the ionization state of an apoprotein moiety with a pK near 9.6. Regardless of which of the above alternatives is assigned as the dominant mechanism for selecting bR_1 versus bR_2, the key proposal is that a small change in protein geometry or binding site electrostatic environment can have a dramatic effect on the primary quantum yield.

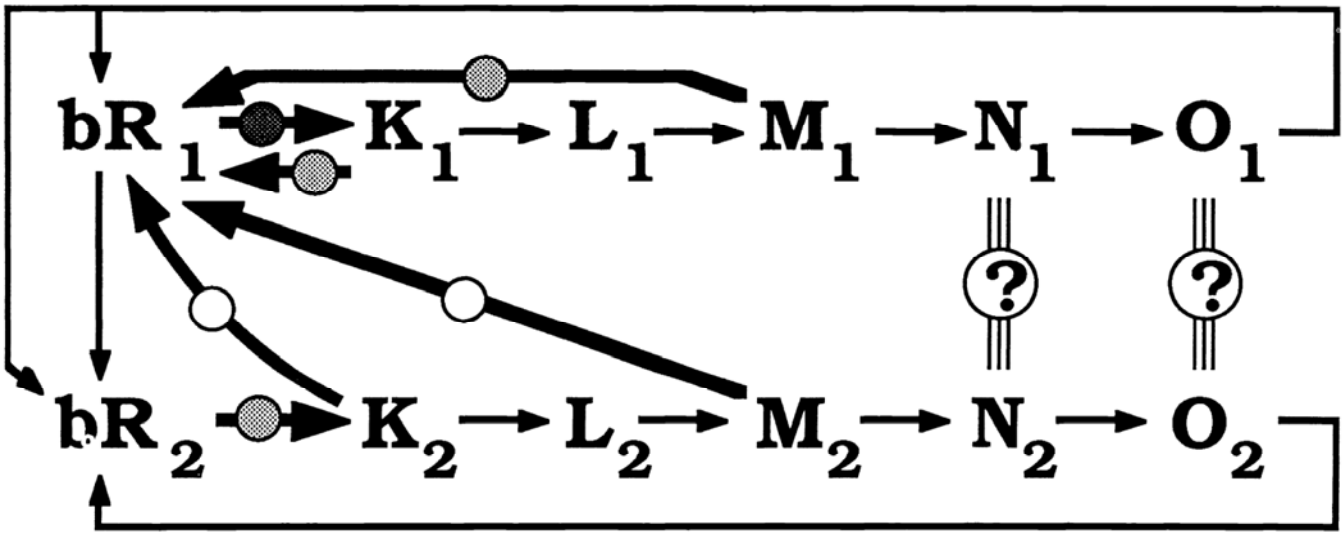

Figure 3. A dual photocycle model of bacteriorhodopsin which rationalizes the experimental observation that *all* direct measurements on Φ_1 yield values greater than or equal to 0.6, while *all* photostationary state measurements on Φ_1 yield values less than or equal to 0.33. The thick arrows indicate photochemical transformations, and the quantum efficiency of the photochemical transformations are indicated by using filled circles: white (Φ unknown), black ($\Phi \sim 0.3$), grey ($\Phi \sim 0.6$). The thin arrows indicate thermal transformations. Thus, the bR_2 photocycle, which has the higher primary quantum yield, is the thermally more stable. Direct measurements will yield high values for Φ_1, because the bR_2—hν→K_2 photoreaction will be selected. However, the back reaction is not K_2—hν→bR_2 but rather K_2—hν→bR_1. Subsequent photochemistry will take place within the bR_1 photocycle, which will select the bR_1—hν→K_1 photoreaction, and yield a lower primary quantum yield. Because the reverse photoreaction from K_1 also selects bR_1, all photostationary measurements will measure the bR_1—hν→K_1 quantum yield, which is ~0.3. It is possible that at some stage in the photocycles, the intermediates of the two photocycles are equivalent (i.e. $N_1 \equiv N_2$, and $O_1 \equiv O_2$). Thus, bR_2 could be formed via thermal relaxation of bR_1 or directly via $O_1 \equiv O_2$.

4.3 Biological relevance

Steady state illumination of intact cells induces the light adapted form of bacteriorhodopsin to eject one or more protons from the cytoplasm generating an electrochemical gradient across the cell membrane. This gradient can be partitioned into two components,[50-52]

$$\Delta p = \Delta\psi - 2.3RT\Delta pH/F \quad (1)$$

$$= \Delta\psi - 59\Delta pH \ (\text{mV at } 25^{\circ}C) \quad (2)$$

where Δp is the proton motive force (or electrochemical gradient), $\Delta\psi$ is the electrical potential difference across the membrane and ΔpH is the pH gradient across the membrane. Eq. 2 is obtained by evaluating RT/F (R = gas constant, F = Faraday constant) at T = 298K. The pH gradient during illumination is dependent upon extracellular pH as well as other factors, and is thus subject to uncertainty. Estimates of ΔpH generally range from 0.7 to 1.5 units (inside alkaline).[52] Estimates of $\Delta\psi$ during illumination generally span the range from -120 to -220 mV.[52] Accordingly, the electrochemical gradient across the cell may reach ~350 mV, but for the purposes of this discussion we will assume an average gradient of 250 mV (= $-\Delta p$).

The free energy required to pump a single proton across a gradient of 250 mV is ~6 kcal mol^{-1} (1 kcal mol^{-1} = 43.4 mV/molecule). For the purposes of this discussion, we will neglect entropy and assume the equivalence of enthalpy and free energy in estimating the relationship between energy storage and proton pumping capability. Under this approximation, the energy stored in the primary event (~16 kcal mol^{-1}) is sufficient to pump two, but not three, protons per photocycle under typical ambient conditions. This maximum stoichiometry is consistent with many of the measurements of proton pumping stoichiometry, which indicate that two protons are pumped per photocycle.[37-40] However, as noted above, environments that select photocycles with primary quantum yields of $\Phi_1 \geq 0.6$ will likely result in a concomitant reduction in energy storage to ~10 kcal mol^{-1} (e.g. Fig. 2). The latter energy storage value is consistent with a proton pumping stoichiometry no larger than one.

It is interesting to speculate on the potential biological relevance of our proposal that two photocycles may exist with different quantum yields and energy storage capacities. For the sake of argument, we will assign these two photocycles to have the following properties:

bR_1 {$\Phi_1 \sim 0.3$, ΔH_{12} ~16 kcal mol^{-1}, [H]/photocycle ~ 2 ($|\Delta p| \leq 250$mV), ~1 ($|\Delta p| > 250$mV)},

bR_2 {$\Phi_1 \sim 0.6$, ΔH_{12} ~10 kcal mol^{-1}, [H]/photocycle ~ 1 ($|\Delta p| \leq 250$mV), ~0 ($|\Delta p| > 250$mV)}.

Following the model presented in Fig. 3, we assign **bR_2** as the lower free energy form of the protein that is nominally active under *in vivo* conditions. Natural selection may have designed bacteriorhodopsin to interconvert from **bR_2** to **bR_1** under conditions of high electrochemical gradient ($|\Delta p| > 250$mV) where **bR_2** is no longer capable of pumping a proton because the free energy stored is insufficient to override the membrane gradient. Because **bR_1** stores more energy in the primary event, it is a more efficient proton pump under conditions of high membrane electrochemical gradient. Analysis of the data of Table I also suggests the possibility that **bR_1** is photochemically selected via reverse photoreactions from **K** or **M**. Thus, under high light intensities, which will result in the generation of high electrochemical gradients, the protein is converted into the most efficient form. While the speculative nature of this discussion should be emphasized, we should not overlook the fact that the unusual photochemical properties of bacteriorhodopsin may have biological relevance.

5. ACKNOWLEDGEMENTS

This work was supported in part by grants from the National Institutes of Health (GM-34548), the National Science Foundation (CHE-8516155), and the Office of Naval Research (N00014-88-K-0359).

6. REFERENCES

1. M. Ottolenghi, *Adv. Photochem.* **12**, 97-200 (1980).
2. R.R. Birge, *Annu. Rev. Biophys. Bioeng.* **10**, 97-200 (1981).
3. W. Stoeckenius and R. Bogomolni, *Annu. Rev. Biochem.* **51**, 587-616 (1982).
4. J.K. Lanyi, in *New Comprehensive Biochemistry*, L. Ernster, ed., pp. 315-350, Elsevier, North Holland, Amsterdam (1985).
5. G.S. Harbison, S.O. Smith, J.A. Pardoen, J. Courtin, J. Lugtenburg, J. Herzfeld, R.A. Mathies and R. G. Griffin, *Biochemistry* **24**, 6955-6962 (1985).
6. J. Lugtenburg, M. Muradin-Szweykowska, C. Heeremans, J. Pardoen, G. Garbison, J. Herzfeld, R. Griffin, S. Smith and R.A. Mathies, *J. Am. Chem. Soc.* **108**, 3104-3105 (1986).
7. J. Spudich, D. McCain, K. Nakanishi, M. Okabe, M. Shimizu, H. Rodman, B. Honig and R. Bogomolni, *Biophys. J.* **49**, 479-483 (1986).
8. R.R. Birge, *Accts.Chem. Research* **19**, 138-146 (1986).
9. K. Schulten and P. Tavan, *Nature (London)* , **272**, 85-86 (1978).
10. M. Engelhard, K. Gerwert, B. Hess, W. Kreitz and F. Siebert, *Biochemistry* **241**, 400-407 (1985).
11. P. Tavan, and K. Schulten, *Biophys. J.* **50**, 81-89 (1986).
12. R. Liu, D. Mead and A. Asato, *J. Am. Chem. Soc.* **107**, 6609 (1985).
13. S. O Smith, I. Hornung, R. van der Steen, J. A. Pardoen, M. S. Braiman, J. Lugtenburg and R. Mathies, *Proc. Natl. Acad. Sci. USA* **83**, 967 (1986).
14. R. R. Birge, T. M. Cooper, A. F. Lawrence, M. B. Masthay, C. Vasilakis, C.F. Zhang and R. Zidovetzki, *J. Am. Chem. Soc.* (in press).
15. R.R. Birge, C.M.Einterz, H.M. Knapp and L.P. Murray, *Biophys. J.* **53**, 367-385 (1988).
16. R.R. Birge, and L.M. Hubbard, *J. Am. Chem. Soc.* **102**, 2195-2205 (1980).
17. R.R. Birge and L.M. Hubbard, *Biophys J.* **34**, 517-534 (1981).
18. J. M. LeClercq and C. Sandorfy, *Photochem. Photobiol.* **33**, 361-65 (1981).
19. R.R. Birge, in *Biological Events Probed by Ultrafast Laser Spectroscopy;* R.R. Alfano, ed., pp. 299-317, Academic Press, New York (1980).
20. W.H. Miller and T.F. George, *J. Chem. Phys.* **56**, 5637-5652 (1972).
21. R.R. Birge, L.A. Findsen and B.M. Pierce, *J. Am. Chem. Soc.* **109**, 5041-5043 (1987).
22. R.R. Birge and T.M. Cooper, *Biophys. J.* **42**, 61-69 (1983).
23. J.B. Hurley and T.G. Ebrey, *Biophys. J.* **22**, 49-66 (1978).
24. C.R. Goldschmidt, O. Kalisky, T. Rosenfeld and M. Ottolenghi, *BiophysJ.* **17**,179-183 (1977).
25. C.R. Goldschmidt, M. Ottolenghi and R. Korenstein, *Biophys. J.* **16**, 839-843 (1976).
26. B. Becher, and T.G. Ebrey, *Biophys. J.* **17**, 185-191 (1977).

27. D. Oesterhelt, P. Hegemann and J. Tittor, *EMBO J.* **4**, 2351-56 (1985).

28. H.-J. Polland, M.A. Franz, W. Zinth, W. Kaiser, E. Kölling and D. Oesterhelt, *Biophys. J.* **49**, 651-662 (1986).

29. D. Oesterhelt and B. Hess, *Eur. J. Biochem.* **37**, 316-326 (1973).

30. R. H. Lozier and W. Niederberger, *Fed. Proc.* **36**, 1805-1809 (1977).

31. T. Iwasa, F. Tokunaga and T. Yozhizawa, *Biophys. Struct. Mech.* **6**, 253-270 (1980).

32. A.K. Dioumaev, V.V. Savransky, N.V. Tkachenko and V.I. Chukharev, *Photochem. Photobiol.* 1988 (in press).

33. H.J.A. Dartnall, in *Handbook of Sensory Physiology*, H.J.A. Dartnall, ed., vol. VII (1972).

34. T. Suzuki and R.H. Callender, *Biophys. J.* **34**, 261-265 (1981).

35. R.R. Birge and R.H. Callender, in *Biophysical Studies of Retinal Pigments*; T. Ebrey, H. Frauenfelder, B. Honig, K. Nakanishi, eds., Univ. Illinois Press, pp. 270-281 (1987).

36. T. Kouyama, A. Nasuda-Kouyama, A. Ikegami, M.K. Methew and W. Stoeckenius, *Biochemistry* **27**, 5855-5863 (1988).

37. T. Marinetti, *Biophys. J.* **51**, 875-881; **52**, 115-121 (1987).

38. T. Marinetti and D. Mauzerall, *Proc. Natl. Acad. Sci. USA* **80**, 178-180 (1983).

39. R.A. Bogomolni, R.A. Baker, R.H. Lozier and W. Stoeckenius, *Biochemistry* **19**, 2152 (1980).

40. R. Govindjee, T.G. Ebrey, and A.R. Crofts, *Biophys. J.* **30**, 231-242 (1980).

41. J.H. Hanamoto, D. Dupois and M.A. El-Sayed, *Proc. Natl. Acad. Sci.U.S.A.* **81**, 7083-7084 (1984).

42. Zs. Dancshazy, R. Govindjee and T.G. Ebrey, *Proc. Natl. Acad. Sci. USA* **85**, 6358-6361 (1988).

43. L.A. Drachev, A.D. Kaulen, V.P. Skulachev and V.V. Zorina, *FEBS Lett.* **209**, 316-320 (1986).

44. J. M. Beach and R. S. Fager, *Photochem. Photobiol.* **41**, 557-562 (1985).

45. O. Kalisky and M. Ottolenghi, *Photochem. Photobiol.* **35**, 109-115 (1982).

46. R. Korenstein, B. Hess and D. Kuschmitz, *FEBS Lett.* **93**, 266-270 (1978).

47. M. Eisenbach, E.P. Bakker, R. Korenstein and S.R. Caplan, *FEBS Lett.* **71**, 228-232 (1976).

48. S.P. Balashov and F.F. Litvin, *Biophysics* **26**, 566-581 (1981).

49. T. Alshuth and M. Stockburger, *Photochem. Photobiol.* **43**, 55-66 (1986).

50. S.J. Ferguson and M.C. Sorgato, *Annu. Rev. Biochem.* **51**, 185-199 (1982).

51. R.R. Birge, A.F. Lawrence, T.M. Cooper, C.T. Martin, D.F. Blair and S.I. Chan, in *Nonlinear Electrodynamics in Biological Systems*, W.R. Adey and A.F. Lawrence, eds. Plenum Publishing, pp 107-120 (1984).

52. J.K. Lanyi, *Microbiol. Rev.* **42**, 682-712 (1978).